



HAL
open science

A non-invasive radar system for automated behavioural tracking: application to sheep

Alexandre Dore, Cristian Pasquaretta, Dominique Henry, Edmond Ricard, Jean-François Bompard, Mathieu Bonneau, Alain Boissy, Dominique Hazard, Hervé Aubert, Mathieu Lihoreau

► To cite this version:

Alexandre Dore, Cristian Pasquaretta, Dominique Henry, Edmond Ricard, Jean-François Bompard, et al.. A non-invasive radar system for automated behavioural tracking: application to sheep. 2021. hal-03438808v1

HAL Id: hal-03438808

<https://hal.science/hal-03438808v1>

Preprint submitted on 4 Jan 2021 (v1), last revised 22 Nov 2021 (v2)

HAL is a multi-disciplinary open access archive for the deposit and dissemination of scientific research documents, whether they are published or not. The documents may come from teaching and research institutions in France or abroad, or from public or private research centers.

L'archive ouverte pluridisciplinaire **HAL**, est destinée au dépôt et à la diffusion de documents scientifiques de niveau recherche, publiés ou non, émanant des établissements d'enseignement et de recherche français ou étrangers, des laboratoires publics ou privés.

1 **A non-invasive radar system for automated** 2 **behavioural tracking: application to sheep**

3
4 Alexandre Dore^{1,2}, Cristian Pasquaretta², Dominique henry¹, Edmond Ricard³, Jean-
5 François Bompard³, Mathieu Bonneau⁴, Alain Boissy⁵, Dominique Hazard³, Hervé
6 Aubert¹, Mathieu Lihoreau²

7
8 ¹ Laboratory for Analysis and Architecture of Systems (LAAS), Toulouse University,
9 CNRS, INPT, F-31400, Toulouse, France

10 ² Research Center on Animal Cognition (CRCA), Center for Integrative Biology (CBI);
11 CNRS, University Paul Sabatier – Toulouse III, France

12 ³ GenPhySE Université de Toulouse, INRAE, ENVT, F-31326 Castanet Tolosan, France

13 ⁴ Guadeloupe INRAE

14 ⁵ UMR Herbivores, Université de Clermont, INRAE, VetAgro Sup, F-63122 Saint-Genès
15 Champanelle, France

16

17 **Abstract**

18

19 Automated quantification of the behaviour of freely moving animals is increasingly
20 needed in ethology, ecology, genetics and evolution. State-of-the-art approaches often
21 require tags to identify animals, high computational power for data collection and
22 processing, and are sensitive to environmental conditions, which limits their large-scale
23 utilisation. Here we introduce a new automated tracking system based on millimetre-
24 wave radars for real time robust and high precision monitoring of untagged animals. To
25 validate our system, we tracked 64 sheep in a standard indoor behavioural test used for
26 genetic selection. First, we show that the proposed radar application is faster and more
27 accurate than conventional video and infrared tracking systems. Next, we illustrate how
28 new behavioural estimators can be derived from the radar data to assess personality
29 traits in sheep for behavioural phenotyping. Finally, we demonstrate that radars can be
30 used for movement tracking at larger spatial scales, in the field, by adjusting operating

31 frequency and radiated electromagnetic power. Millimetre-wave radars thus hold
32 considerable promises for high-throughput recording of the behaviour of animals with
33 various sizes and locomotor modes, in different types of environments.

34
35 Keywords: computational ethology, radar tracking, behavioural phenotyping, *Ovis aries*,
36 corridor test.

37

38 **1. Introduction**

39

40 Animal behaviour research increasingly requires automated recording and analyses of
41 movements (Branson et al., 2009). The emerging field of computational ethology
42 provides methods for high-throughput monitoring and statistical analyses of movements
43 that enable the quantitative characterisation of behaviour on large numbers of
44 individuals, the discovery of new behaviours, but also the objective comparison of
45 behavioural data across studies and species (Anderson and Perona, 2014; Brown and
46 de Bivort, 2018).

47 These quantitative approaches are particularly powerful to study inter-individual
48 behavioural variability or personalities in animal populations (Morand-Ferron et al.,
49 2015). In livestock, for instance, large-scale genetic selection programmes are based on
50 the measurements of several hundreds (if not thousands) of farm animals (O'Brien et al.
51 2014). Many behavioural tests have been developed to assess behavioural and
52 personality traits in farm animals (Canario et al. 2013), and some applications have
53 been developed in breeding programmes for instance to discard the more aggressive
54 individuals for beef cattle production (Phocas et al. 2006). Behavioural measures are
55 frequently obtained from direct observations by the experimenters or farmers (e.g.,
56 Boissy et al., 2005), limiting use of behavioural criteria for breeding programmes.
57 Indeed, the absence of automated measurements make data collection cumbersome,
58 time-consuming and prone to biases, which currently limits the ability to quantify
59 behavioural traits at the experimental or commercial farm level.

60 Tracking methods involving on-board devices, such as Global Positioning
61 Systems (GPS) (Tomkiewicz et al., 2010), radio telemetry (Cadahia et al., 2010), radio

62 frequency identification (RFID) (Voulodimos et al., 2010) or harmonic radar (Riley et al.,
63 1996), are hardly suitable for detailed high throughput behavioural phenotyping due to
64 the limited accuracy and duration of measurements. Best available methods therefore
65 involve image-based analyses (Pérez-Escudero et al., 2014; Romero-Ferrero et al.,
66 2019). However, these techniques often require large computational resources to
67 acquire and process images (Garcia et al 2019) and are sensitive to light variation (Dell
68 et al., 2014).

69 Recently, Frequency-Modulated Continuous-Wave (FMCW) radars operating in
70 the millimetre-wave frequency band have been proposed for automated tracking of
71 animal behaviour (sow: Dore et al., 2020b, bees: 2020a; sheep: Henry et al., 2018). In
72 this approach, it is possible to record the 1D movements (distance to radar) of individual
73 sheep in an arena test (Henry et al., 2018). Tracking with FMCW radars has the great
74 advantage of being non-invasive (does not require a tag), insensitive to light intensity
75 variations, and fast (as it does not require large memory resource). FMCW radars
76 therefore provide considerable advantages for the development of automated high-
77 throughput analyses in regard to more conventional approaches (e.g. video and infrared
78 tracking systems).

79 Here we developed a millimetre-wave FMCW radar system for automated
80 tracking and analyses of the 2D trajectories of freely moving animals. We illustrated our
81 approach by analysing the behaviour of 64 sheep in an “arena test” commonly used to
82 estimate the sociability of individual sheep in genetic selection (Boissy et al., 2005;
83 Hazard et al., 2014). First, we compared the speed and accuracy of radar tracking with
84 more conventional video and infrared tracking systems. We then derived new
85 behavioural estimators computed from the radar data, that could be used for large-scale
86 behavioural phenotyping. Finally, we tested the radar system for long-distance tracking,
87 in the field, by adjusting radar emission frequency and radiated electromagnetic power.

88

89 **2. Materials and methods**

90

91 **Sheep**

92

93 We ran the experiments in July 2019 at the experimental farm La Fage of the French
94 National Research Institute for Agriculture, Food, and Environment (INRAE), France
95 (43.918304, 3.094309). We tested 64 lambs (32 males, 32 females) *Ovis aries* with
96 known weight (range: 12kg – 31.3kg) and age (range: 59 days – 88 days). Ewes and
97 their lambs were reared outdoor on rangelands. After weaning, lambs were reared
98 together outside and tested for behaviour 10 days later. This delay allowed the
99 development of social preferences for conspecifics instead of preference for mother. All
100 the lambs were previously tested in a “corridor test” to estimate their docility towards a
101 human. Briefly the test pen consisted of a closed, wide rectangular circuit (4.5 x 7.5 m)
102 with opaque walls (Boissy et al., 2005). A non-familiar human entered the testing pen
103 and moves at constant speed through the corridor until two complete tours had been
104 achieved. Every 5 s (i.e. the corridor was divided into 6 virtual zones and 1 zone was
105 crossed every 5 s by the human) the zones in which the human and the animal were
106 located were recorded and the mean distance separating the human and the lamb was
107 calculated. The walking human also recorded with a stopwatch the total duration when
108 the human saw the head of the lamb to discriminate between fleeing and following
109 lambs. The reactivity criteria towards an approaching human was constructed by
110 combining both measurements (for more details see Hazard et al., 2016). The higher
111 was the resulting variable (i.e. docility variable), the more docile was the animal.

112

113 **Arena test**

114

115 We tested all the sheep in the arena test, a standard protocol for assessing the
116 sociability of sheep through measures of inter-individual variability in social motivation in
117 the absence or presence of a shepherd (Boissy et al., 2005; Hazard et al., 2014). Briefly,
118 a sheep (focal sheep) was introduced in the pen (2mx7m) with artificial lights (Fig. 1A;
119 for more details see Ligout et al. 2011). Three other sheep from the same cohort (social
120 stimuli) were placed behind a grid barrier, on the opposite side of the corridor entrance.
121 The test involved three phases (Fig. 1B). In phase 1, the focal sheep could explore the
122 corridor for 15s and see its conspecifics through a grid barrier. In phase 2, visual contact
123 between the focal sheep and the social stimuli was disrupted using an opaque panel

124 pulled down from the outside of the pen. This phase was used to assess the sociability
125 of the sheep towards its conspecifics and lasted 60s. In phase 3, visual contact between
126 the focal sheep and its conspecifics was re-established and a man was standing still in
127 front of grid barrier for 60s. This phase was used to assess the sociability of the focal
128 sheep towards conspecifics in presence of a motionless human.

129

130 **Data collection**

131

132 We measured the displacement of the focal sheep in phases 2 and 3 of the arena test
133 (phase 1 is the initiation phase) using three automated tracking systems: infrared
134 sensors, a video camera, and a millimetre-wave FMCW radar. During the measures, an
135 experimenter also recorded the number of high-pitched bleats by the focal sheep, a
136 proxy of the sociability (i.e. sociability variable) of the sheep (Boissy et al., 2005).

137

138 Tracking with infrared cells

139

140 Infrared cells were previously used to quantify sheep behaviour in the arena test. We
141 placed two infrared sensors every meter along the arena length (Fig. 1A). We used two
142 infrared sensors to determine the direction of the moving sheep. The focal sheep was
143 recorded each time it passed through one of these sensors. Sheep movements were
144 thus tracked in 1D (longitudinal movements in the corridor) and data resolution was 1m.

145

146 Video tracking

147

148 We placed a video camera on one end of the arena (opposite to entrance side, Fig. 1B).
149 The camera was elevated 2m above ground in order to film the entire arena. Sheep
150 movements were tracked in 2D. For image processing, we applied a detection algorithm
151 using the state-of-the-art image object detector tiny-YOLO (You Only Look Once)
152 network, which is a version of the YOLO model adapted for faster processing allowing
153 244 images of 0.17 mega pixels (416 x 416 pixels) per second (on a TITAN X graphics

154 card) (Redmon et al., 2016). This neural network was pre-trained on the PASCAL Visual
155 Object Classes Challenge dataset (Everingham et al., 2012).

156

157 Radar tracking

158

159 We placed a millimetre-wave FMCW radar (Fig. 1C, see technical characteristics in
160 Table 1) at one end of the arena (entrance side, Fig. 1B). The radar was setup outside
161 of the test pen behind a Styrofoam wall transparent to millimetre-wave (Dietlein et al.,
162 2008). The transmitting antenna array radiated a repetition over time of a so-called chirp
163 (i.e. a saw-tooth frequency-modulated signal (Balanis, 2011)). The chirp was
164 backscattered by the targeted focal sheep, but also by the surrounding scene which
165 provides undesirable radar echoes called the electromagnetic clutter. The total
166 backscattered signal was then collected by the receiving antenna array and processed
167 to mitigate the clutter and to derive the sheep 2D trajectory from radar data. In the
168 millimetre-wave frequency range, the detectability of the sheep depends mainly on the
169 bandwidth of the frequency modulation, the beamwidth of the radar antennas, and the
170 radiated electromagnetic power (Balanis, 2011)).

171

172 **Radar signal processing**

173

174 Processing of radar data included two main steps. First, we extracted the position of the
175 animal. Next, we computed behavioural parameters to characterize the movement of the
176 animal.

177

178 Extraction of sheep positions

179

180 We extracted the distance of the focal sheep to the radar and its direction in the
181 horizontal plane of the scene. To mitigate the electromagnetic clutter, we estimated the
182 mean value (*mean*) and standard deviation (*std*) of the signal provided by the radar in
183 absence of the sheep and derived the signal $Detection(r, \theta)$ from the signal $S_{radar}(r, \theta)$
184 delivered in presence of the animal, as follows:

$$Detection(t, r, \theta) = \frac{S_{radar}(t, r, \theta) - mean(r, \theta)}{std(r, \theta)}$$

185 Where r is the distance to the sheep, *mean* is the time-averaged signal radar coming
186 from the range r and angular position θ , *std* is the time-standard deviation of the radar
187 signal. Fig. 1D shows an example of position estimations of a sheep over time after
188 removing the clutter.

189

190 Extraction of new behavioural parameters

191

192 From the 2D trajectory data, we extracted new behavioural parameters to characterize
193 sheep movements using three approaches.

194

195 *Computation of behavioural classes*

196

197 We statistically identified broad classes of behaviour using automated classification.
198 First, we extracted movement parameters (speed, sinuosity and speed of displacement)
199 from the trajectories. Then, to differentiate the movement modifying the distance of the
200 sheep from the social stimuli (i.e. the three conspecifics) and a lateral movement, the
201 speed vector was split in two dimensions: along the two lateral walls of the corridor and
202 across the two longitudinal walls. These characteristics were estimated on time windows
203 of 1s for each sheep and for each experimental phase. Finally, to derive behavioural
204 classes, we performed an extraction from a Gaussian mixture model using the extracted
205 data for each lamb (Reynolds and Rose, n.d.). The number of classes (i.e. the number

206 of Gaussians to be used) was determined by comparing models using 1 to 15 classes.
207 We selected the model with the lowest Akaike score which represents the model with
208 the features best explaining the parameter under consideration (Burnham and
209 Anderson, 2002).

210

211 *Computation of behavioural transitions*

212

213 We determined behavioural changes over time using Ricker wavelet processing (Ryan,
214 1994; see examples Fig. 3). Wavelet processing consists in filtering the sheep position
215 signal using a wavelet as a filter (Poirier et al., 2009). This type of filtering is applied to
216 several time scales, thus allowing the detection of a behaviour regardless of how long
217 this behaviour lasts. Our aim was to determine the precise moments when the focal
218 sheep changed its moving behaviour, which was estimated using the spectrum
219 described by each wavelet. We observed that the number of local maxima in the wavelet
220 transform coefficients is sensitive to the number of behaviour changes (see example in
221 Fig. S1B).

222

223 *Computation of space coverage*

224

225 We investigated the space occupied across time by the focal sheep using heatmaps
226 (see examples Fig. 4). We partitioned the arena into 80 zones of 44x40cm each (i.e. 16
227 partitions along the arena length and 5 partitions along the arena width). We chose this
228 zone dimension because it corresponded to the width of a small lamb (Idris et al., 2011).
229 We counted the number of zones the focal sheep remained in for more than 200ms. We
230 considered that a lamb stayed in a given zone for less than 200ms either because it was
231 positioned at the edge of this zone or because the estimation of position by the radar
232 was inaccurate (this situation occurred for less than 10% of detections).

233

234 **Outdoor radar tracking**

235

236 We ran outdoor experiments in order to demonstrate the applicability of our radar
237 system for long-range tracking of sheep (Fig. 4). These measurements were done in
238 an open space with no obstacles (60m x 15m). A man moved in order to induce animal
239 movements. We tested one female sheep (2 years, 60 Kg). To enhance detection range
240 to 40 m, we used a FMCW radar with a lower operating frequency (24GHz; (Simon et
241 al., 2014)). At constant transmitted power, lower frequencies enable to reduce the free-
242 space attenuation of the radiated electromagnetic power (Balanis, 2011). We used the
243 same signal processing as with the 77GHz radar.

244

245 **Statistical analyses**

246

247 We ran all analyses using the programming environment R (R Core Team, 2014). Raw
248 trajectory data extracted from radar and video measures are available in Dataset S1.

249

250 Comparison of the performances of the different tracking systems

251

252 We tested the ability of radar and video tracking systems to capture the same
253 information as the infrared cells from the computation of two parameters: (1) a crossing
254 rate and (2) a proximity score (respectively LOCOM and PROX in Hazard et al. 2014).
255 The crossing rate is the number of times the animal moved between virtual zones
256 defined by the infrared cells (1x2m) without distinguishing between the zones nor the
257 direction of movement. This rate thus provides information on the displacement activity
258 of animals seeking contact with their conspecifics. The proximity score is the total
259 duration the focal sheep remained in each zone weighted as the animal moves closer to
260 its conspecifics. The weight depends on the distance between the sheep and the
261 conspecifics:

$$w_i = \frac{1}{i}$$

262 with w_i the weight of the zone considered, i the index of the zone delimited by the
263 infrared sensors. $i = 1$ corresponds to the zone close to the conspecifics, and $i = 7$
264 corresponds to the zone close to the corridor entrance. Thus, an animal with a high
265 proximity score spent more time close to its conspecifics. We calculated these two

266 parameters from data collected from infrared cells, video and radar tracking systems
267 and compared them using Pearson's correlation tests (using 'stats' R package).

268 We compared the accuracy of radar and video data systems by running a general
269 linear mixed model (GLMM using glmer function in 'lme4' R package (Bates et al.,
270 2014)) testing the effect of the tracking method on the proportion of false detections,
271 with sheep identity as random factor. We estimated the correlation between the number
272 of false detections with the two methods using the Pearson's correlation test.

273

274 Analyses of new movement features

275

276 We tested the influence of the sheep characteristics on behavioural classes using
277 generalised models (GLMMs). Models (binomial family) tested the effects of phase,
278 docility, weight, age, sociability, sex, and dual interactions of each variable with test
279 phase, on the proportion of time spent in fast movements (behavioural class 2).
280 Interactions between more than two variables were excluded because of the high
281 number of variables relative to sample size. Sheep identity was included as a random
282 factor. We ran a model selection by using all features combinations (age, weight,
283 docility, sociability, sex and the phase when the radar measurement was done). We kept
284 the model with the highest Akaike score. We used a similar procedure to test the
285 influence of the sheep characteristics of the lambs on continuous wavelet transforms
286 (Gaussian models) and heatmaps (Poisson models). For the continuous wavelet
287 transform, we performed two different wavelet transforms on the lateral and on the
288 longitudinal position of the sheep. For heatmaps, we tested different grid resolutions
289 characterised by zone sizes: a low resolution grid with 21 zones (3 x 7) and a high
290 resolution grid with 45 zones (5 x 15).

291

292 Classification of behavioural types

293

294 To classify sheep from on our new behavioural estimators, we ran a principal
295 component analysis (PCA) based on the eight behavioural measures extracted from the
296 radar data in phase 2 and phase 3: proportion of fast movements (class 1) out of all

297 movements (class 1 + class 2), longitudinal movements (wavelets Y), latitudinal
298 movements (wavelets X), space coverage (heatmaps).

299

300 **3. Results**

301

302 **Radar tracking is more faster and more accurate than video tracking**

303

304 To validate the radar tracking system, we compared the data obtained from the infrared
305 cells, video and radar. We analysed data from 58 (29 males, 29 females) out of the 64
306 sheep initially tested, because some recordings failed during measurements due to
307 human errors or miss detection by infrared cells.

308 Both data collected by radar and video enabled to capture information given by
309 infrared cells with high fidelity. Proximity scores and crossing rates obtained from
310 infrared cells were positively correlated with data obtained from radar (Pearson
311 correlation; proximity: $r = 0.77$, $p < 0.001$; crossing rate: $r = 0.87$, $p < 0.001$) and video
312 (Pearson correlation test; proximity: $r = 0.91$, $p < 0.001$; crossing rate: $r = 0.34$, $p =$
313 < 0.001). Imperfect correlation between proximity scores and crossing rates obtained
314 from different tracking methods are caused by the different reference points used for
315 tracking: infrared cells detect the full body of the sheep, whereas image analysis detects
316 the centre of mass of the sheep, and the radar detects body parts of the sheep that are
317 closest to it.

318 The comparison between the radar and the video data showed both tracking
319 systems involved low levels of false detections (i.e. when the distance between the body
320 centre of the sheep and its estimated position is greater than one sheep body length).
321 However, radar tracking generated ca. three times less false detections than video
322 tracking (Binomial GLMM, $z = -3.595$, $p < 0.001$; Table 2). False detection with the two
323 methods had different origins. False video detections resulted from insufficient colour
324 contrast between the lamb and the background (e.g. when the lamb was close to the
325 wall of the corridor), whereas false radar detections resulted from the low angular
326 resolution of the radar and potential multiple reflections of the transmitted
327 electromagnetic signal by obstacles in the scene (such as walls, ground, human). Radar

328 and video tracking systems are therefore complementary. The combination of the two
329 systems gave the exact position of the sheep in 97.83% of the measures.

330 Radar tracking had additional advantages over video tracking in terms of data
331 processing (Table 2). The radar produced two times more measures per second. Radar
332 processing was also much faster and therefore it may be used for real time data
333 analyses. Radar measures were of similar size as video measures (ROM), but required
334 ca. 7 times less memory (RAM) to process. Finally, radar processing did not require a
335 learning phase with important data collection and a time-consuming training phase that
336 can last several hours just for the adaptation of the model, or several days if the network
337 is not trained beforehand.

338

339 **New behavioural indicators from radar data**

340

341 The following analyses were made on the 64 sheep tested (32 males, 32 females). The
342 obtained 2D trajectory data offered the opportunity for high resolution analyses of sheep
343 movements.

344

345 Behavioural classes: detection of slow and fast movements

346

347 We applied a Gaussian Mixture Model (GMM) procedure to statistically identify
348 behavioural classes from the 2D trajectory data. We found four behavioural classes (Fig.
349 2A). Class 1 (51.3% of measures) was characterized by null or slow movements (“slow
350 movements”). Class 2 (35.48% of measures) was characterized by fast movements with
351 low sinuosity (“fast movement”). Class 3 (10.2% of measures) was characterized by fast
352 movements with high sinuosity (“fast tortuous”). Class 4 (3.01% of measures) was
353 characterized by slow movements with high sinuosity (“slow tortuous”). Each of the two
354 behavioural classes with strong sinuosity (classes 3 and 4) represented less than 10%
355 of all data. We thus focused our analyses on slow and fast movements (classes 1 and
356 2).

357 We tested the effects of the individual characteristics of sheep on time spent in
358 each behavioural class using GLMMs. Results of the best model (i.e. highest Akaike

359 score) are summarized in Table 3 (see model selection in Table S1). Male, old, large
360 and highly docile sheep spent significantly more time in slow movement during phase 3
361 than during phase 2 (Fig. 2C). Highly sociable sheep also spent more time in slow
362 movements during phase 3 than during phase 2 (Fig. 2D).

363

364 Wavelet analyses: detection of erratic behavioural transitions

365

366 We quantified behavioural changes during time (variation in speed, direction, or both)
367 using continuous wavelet analyses. We tested the effects of the individual
368 characteristics of sheep on the frequency of behavioural changes using GLMMs and
369 model selection (Tables S2 and S3). When considering longitudinal movements along
370 the corridor length (Table 4A), we found that males made more behavioural transitions
371 in phase 3 than in phase 2. Highly sociable sheep made more behavioural transitions in
372 phase 3 than in phase 2 (Fig. 3A). When considering latitudinal movements along the
373 corridor width (Table 4B), we found that highly docile sheep made more behavioural
374 transitions in phase 3 than in phase 2 (Fig. 3B). Thus overall, wavelet analyses of
375 longitudinal movements can be used as a proxy of sociability, and analyses of latitudinal
376 movements give information about docility.

377

378 Heatmap analyses: Detection of occupied space

379

380 We quantified spatial coverage by individual sheep (number of zones occupied in the
381 corridor) using heatmaps. We tested the effects of the individual characteristics on the
382 number of zones in which the sheep spent more than 200ms using GLMMs and model
383 selection (Tables S4 and S5). When considering a grid with low spatial resolution, i.e.
384 similar zone dimensions as with infrared cells (i.e., dimension: 0.6 x 1m; example Fig.
385 4A), we found that sheep used 2.37 times less space in phase 3 than in phase 2 (Table
386 5A). Larger individuals used more space than smaller ones (Table 5A). Increasing the
387 spatial resolution of the grid, i.e. similar zone dimension as a lamb body size (i.e.
388 dimension: 0.44 x 0.40 m; example Fig 4A), revealed that highly docile sheep used more
389 space in phase 3 than in phase 2 (Table 5B). Young and highly social individuals used

390 more space than old and poorly social individuals in both phases. Body size effect,
391 however, was not significant anymore. Therefore, heatmap analyses are sensitive to
392 grid size resolution. Decreasing grid size increased behavioural resolution.

393

394 **Sheep behavioural phenotype**

395

396 We explored whether the new behavioural measures extracted from the radar data
397 could capture information from behavioural traits measured manually by the
398 experimenter in the corridor test. We focused on docility and sociability.

399 We ran a PCA based on the eight behavioural measures extracted from the radar
400 data in phase 2 and phase 3: proportion of fast movements (class 1) out of all
401 movements (class 1 + class 2), longitudinal movements (wavelets Y), latitudinal
402 movements (wavelets X), space coverage (heatmaps). We retained two PCs using the
403 Kaiser-Guttman criterion (Kaiser, 1991). PC1 explained 36% of the variance and PC2
404 explained 22% of the variance. PC1 was positively associated with all behavioural
405 variables (Fig. 5A). Sheep with high PC1 values moved more often faster, made more
406 behavioural transitions, and used more zones than sheep with low PC1 values. We
407 therefore interpreted PC1 as a “movement speed” variable. PC2 was positively
408 associated with the four behavioural variables of phase 3 and negatively associated with
409 the four behavioural variables of phase 2 (Fig. 5A). Sheep with high PC2 values showed
410 a more important increase of time spent moving fast, of the frequency of behavioural
411 transitions, and numbers of zones occupied from phase 2 to phase 3 than sheep with
412 low PC2 levels. We interpreted PC2 as a variable of “movement increase between
413 phases”.

414 Sociability was significantly explained by PC1 (LM, PC1: estimate = 0.027, t =
415 2.552, p = 0.014; PC2: estimate = -0.104, t = -0.764, p = 0.448; Fig. 5B). Docility was
416 significantly explained by PC2 (LM, PC1: estimate = -0.081, t = -0.943, p = 0.350; PC2:
417 estimate = 0.283, t = 2.547, p = 0.014; Fig. 5C). Therefore, the automatically extracted
418 radar data can capture inter-individual variability in sociability and docility traits usually
419 measured by experimenters.

420

421 **Outdoor radar tracking**

422
423 To demonstrate that our tracking system can be used in various experimental contexts,
424 we tracked sheep in an outside corridor at a larger spatial scale (10 x 60m; Fig. 6A). We
425 monitored the 2D trajectory of one sheep over a maximum distance of 45m (Fig. 6B).
426 The presence of the man to induce sheep movement did not impair tracking (Fig. 6C).

427

428 **Discussion**

429
430 Research in behaviour and ecology increasingly requires automated monitoring and
431 annotation of animal movements for comparative quantitative analyses (Anderson and
432 Perona, 2014; Brown and de Bivort, 2018). Here we introduced a radar tracking system
433 suitable to study the 2D movements of sheep within a range of 45 m. The system is non-
434 sensitive to light variations, compatible with real time data analyses, transportable, fast
435 processing and adaptable to various species and experimental contexts. Moreover, it
436 does not require to use tags or transponders for tracking the animals. It is therefore
437 suitable for the collection of large sets of behavioural data in an automated way required
438 in many areas of biological and ecological research.

439 FMCW radars were recently used to track sheep and pigs in 1D (Dore et al.,
440 2020b; Henry et al., 2018) and bees in 3D (Dore et al., in press). Here, for the first time,
441 we demonstrate the applicability of this approach to monitor 2D trajectories of untagged
442 walking animals within a range of 45 meters with high spatial resolution. Radar
443 acquisition system has several advantages over more conventional methods, and in
444 particular video tracking, as it collects more data per seconds, requires less RAM, less
445 processing time (e.g. does not require to train neural networks) and generates less false
446 detection rates. It can therefore be applied for real-time detection of animal position.
447 Importantly, the radar is not dependent on brightness and can be used for outside
448 tracking over long distances by adjusting operating frequencies. It also enables the
449 tracking of individualised animals without tags, based on the size and shape of the radar
450 echoes of the different targets. Others methods can be used to estimate the sheep
451 position. The main two methods are video detection (Bonneau et al., 2020), which can

452 detect sheep in 2D up to 25m but with a precision of about 2m, and GPS detection
453 (Gwyn et al., 1995), but this requires to animals.

454 Our application of radar-based tracking to behavioural phenotyping of sheep
455 shows that the radar analysis is consistent with current manual or semi-automated
456 analyses. we found that sheep tend to have a greater displacement in phase 2 than in
457 phase 3 of the corridor test. This is consistent with previous work showing that sheep
458 are more active when socially isolated, presumably as the result of them searching for
459 social contact with conspecifics. These docile animals tend to move less when they are
460 in contact with men. Importantly, the high resolution 2D trajectories obtained from the
461 radar enabled to identify new behavioural estimators that could greatly benefit the fast
462 and automated identification of behavioural phenotypes. These different estimators are
463 not dependent on the radar tracking system per se, but requires to detect the position of
464 the sheep with sufficient time resolution. For example, our application of unsupervised
465 behavioural annotation to identify statistically significant behaviours by sheep in the
466 corridor test showed that sheep exhibit less fast movements in phase 3 than in phase 2.
467 Our utilisation of wavelet analyses revealed the occurrence of erratic displacements.
468 The more the sheep was sociable the more it made erratic longitudinal movements. The
469 more the sheep was docile, the more it made erratic latitudinal movements. We also
470 analysed space occupation by sheep, showing that individuals exploit narrower areas in
471 phase 3 than in phase 2. All these results are consistent with previous observations
472 using manual or semi-automated recording methods. Most importantly, the combination
473 of these new automatically computed estimators appears to be correlated with
474 behavioural traits of interest that were until now measured manually by an experimenter
475 during the corridor test or in complementary tests (e.g. carousel test). Therefore, in
476 principle, our automated tracking and analysis system can be used for automated
477 classification of animal behavioural profiles, which is a major issue for mass phenotyping
478 in animal selection (Beausoleil et al., 2012). Note however that our pioneering study is
479 based on relatively low sample sizes (64 individuals) and further measurements are
480 needed to verify the biological trends observed on a much larger number of sheep.

481 Beyond genetic selection of farm animals, our system can be tuned to suit a large
482 diversity of animal sizes and experimental contexts. Range and resolution of detection

483 can be improved using different radars. For instance, we had to placed the radar at 1
484 meter from the corridor in order to track the entire corridor area. But with other antennas
485 and a radar with larger field of view could have been placed at the edge of the corridor.
486 Moreover, the detection was limited to a few meters but it is possible to detect a sheep
487 at tens of meters using a radar operating at a lower frequency (24GHz) and/or
488 transmitting higher electromagnetic power. It is also possible to improve radar detection
489 by using more antennas. Indeed, by multiplying the number of antennas, we multiply the
490 number of signal estimations and then the noise from the radar can be decreased. In the
491 future, the same radar technology could be used to track individuals in groups over
492 longer distances in open fields, for instance to explore the mechanisms underpinning
493 social network structures and collective behaviour (Ginelli et al., 2015; King et al., 2012).
494 Furthermore, it is possible to improve the processing of the radar signal for tracking
495 large number of sheep simultaneously by using deep radar processing but this would
496 require the use of a large amount of annotated data to train the neural networks (Huang
497 et al., 2018). Individual tracking within groups could be improved with non-invasive
498 passive tags that depolarize radar signal in specific directions (Lui and Shuley, 2006).

499 To conclude we demonstrate the feasibility of tracking a sheep in a restricted
500 area using a FMCW radar. This detection is possible even if each wall of the corridor
501 backscatters the transmitted electromagnetic signal. This radar can also be
502 advantageously used to extract features that are relied to the movement of the sheep
503 and can estimate if it is erratic, fast and the space occupied in the corridor. In contrast to
504 other short-range methods, this 2D detection method does not require pre-annotated
505 data and can be applied in real time. This flexibility holds considerable premises for
506 tracking the behaviour of animals of various sizes and environments in a wide range of
507 contexts and research fields.

508

509 **Acknowledgements**

510

511 AD was funded by a PhD fellowship from the Council of the Région Occitanie (SIDIPAR
512 Project). HA and ML also received support from grant of the French National Research
513 Agency (ANR-DFG 3DNavibee; ANR TERC BEE-MOVE).

514

515 **References**

- 516 Anderson, D.J., Perona, P., 2014. Towards a science of computational ethology. *Neuron* 84, 18–
517 31.
- 518 Balanis, C.A., 2011. *Modern antenna handbook*, John Wiley&Sons. ed.
- 519 Bates, D., Maechler, M., Bolker, B., Waleker, S., 2014. *lme4: linear mixed-effects models using*
520 *Eigen and S4*. R package version 1.
- 521 Beausoleil, N.J., Blache, D., Stafford, K.J., Mellor, D.J., Noble, A.D.L., 2012. Selection for
522 temperament in sheep: Domain-general and context-specific traits. *Applied Animal Behaviour*
523 *Science* 139.
- 524 Boissy, A., Bouix, J., Orgeur, P., Poindron, P., Bibe, B., Le Neindre, P., 2005. Genetic analysis
525 of emotional reactivity in sheep: effects of the genotypes of the lambs and of their dams. *Genetics*
526 *Selection Evolution* 37, 381–401.
- 527 Bonneau, M., Vayssade, J.A., Troupe, W., Arquet, R., 2020. Outdoor animal tracking combining
528 neural network and time-lapse cameras. *Computers and Electronics in Agriculture* 168.
- 529 Branson, K., Robie, A.A., Bender, J., Perona, P., Dickinson, M.H., 2009. High-throughput
530 ethomics in large groups of *Drosophila*. *Nat Methods* 6, 451–457.
- 531 Brown, A.E.X., de Bivort, B., 2018. Ethology as a physical science. *Nat Phys* 14, 653–657.
- 532 Burnham, K.P., Anderson, D.R., 2002. *Model selection and multimodel inference: a practical*
533 *information-theoretic approach*, 2nd Edition. ed. Springer, New York, NY.
- 534 Cadahia, L., López-López, P., Urios, V., Negro, J.J., 2010. Satellite telemetry reveals individual
535 variation in juvenile Bonelli's eagle dispersal areas. *European Journal of Wildlife Research* 56.
- 536 Canario, L., Mignon-Grasteau, S., Dupont-Nivet, M., Phocas, F., 2013. genetics of behavioural
537 adaptation of livestock to farming conditions. *Animal* 7, 357-377.
- 538 Dell, A.I., Bender, J.A., Branson, K., Couzin, I.D., de Polavieja, G.G., Noldus, L., Pérez-
539 Escudero, A., Perona, P., Straw, A.D., Wikelski, M., Brose, U., 2014. Automated image-based
540 tracking and its application in ecology. *Trends Ecol Evol* 29, 417–428.
541 <https://doi.org/10.1016/j.tree.2014.05.004>
- 542 Dietlein, C.R., Bjarnason, J.E., Grossman, E.N., Popovic, Z., 2008. Absorption, transmission, and
543 scattering of expanded polystyrene at millimeter-wave and terahertz frequencies. *Passive*
544 *Millimeter-Wave Imaging Technology XI* 6948–69480.
- 545 Dore, A., Henry, D., Aubert, H., Lihoreau, M., 2020a. 3D trajectories of multiple untagged flying
546 insects from millimetre-wave beamscanning radar. Presented at the IEEE International
547 Symposium on Antennas and Propagation and North American Radio Science Meeting, Québec,
548 Canada.
- 549 Dore, A., Henry, D., Aubert, H., Lihoreau, M., in press. 3D trajectories of multiple untagged
550 flying insects from millimetre-wave beamscanning radar. *IEEE Antennas and Propagation*.
- 551 Dore, A., Lihoreau, M., Billon, Y., Ravon, L., Reignier, S., Bailly, J., Bompa, J.F., Ricard, E.,
552 Aubert, H., Henry, D., Canario, L., 2020b. Millimeter-wave Radars for the Automatic Recording
553 of Sow Postural Activity. Presented at the 71st Annual Meeting of European Federation of
554 Animal Science, Porto, Portugal.
- 555 Everingham, M., Van Gool, L., Williams, C.K.I., Winn, J., Zisserman, A., 2012. Results 2012.
556 *The PASCAL Visual Object Classes Challenge 2012 (VOC2012)*.
- 557 Ginelli, F., Peruani, F., Pillot, M.H., Chaté, H., Theraulaz, G., Bon, R., 2015. Intermittent
558 collective dynamics emerge from conflicting imperatives in sheep herds. *Proc Natl Acad Sci*

- 559 USA 112, 12729–12734.
- 560 Gwyn, R., Williams, A., Last, J.D., Penning, P.D., Mark Rutter, S., 1995. A Low-Power
561 Postprocessed DGPS System for Logging the Locations of Sheep on Hill Pastures. *Navigation*
562 42.
- 563 Haderer, A., Wagner, C., Feger, R., Stelzer, A., 2008. A 77-GHz FMCW front-end with FPGA
564 and DSP support, in: 2008 International Radar Symposium. pp. 1–6.
- 565 Hazard, D., Moreno, C., Foulquié, D., Delval, D., François, D., Bouix, J., Sallé, G., Boissy, A.,
566 2014. Identification of QTLs for behavioral reactivity to social separation and humans in sheep
567 using the OvineSNP50 BeadChip. *BMC Genomics* 15, Artilece 778.
- 568 Hazard, D., Bouix, J., Chassier, M., Delval, E., Foulquié, D., Fossier, T., Bourdillon, Y.,
569 François, D., Boissy, A., 2016. Genotype by environment interactions for behavioral reactivity in
570 sheep. *J Anim Sci* 94, 1459-1471.
- 571 Henry, D., Aubert, H., Ricard, E., Hazard, D., Lihoreau, M., 2018. Automated monitoring of
572 livestock behavior using frequency-modulated continuous-wave radars. *Prog Electromagn Res* 69,
573 151–160.
- 574 Huang, H., Gui, G., Sari, H., Adachi, F., 2018. Deep learning for super-resolution DOA
575 estimation in massive MIMO systems. Presented at the IEEE 88th Vehicular Technology
576 Conference (VTC-Fall).
- 577 Idris, A., Moors, E., Budnick, C., Herrmann, A., Erhardt, G., Gauly, M., 2011. Is the
578 establishment rate and fecundity of *Haemonchus contortus* related to body or abomasal
579 measurements in sheep? *Animal* 5, 1276–1282.
- 580 Kaiser, H.F., 1991. Coefficient alpha for a principal component and the Kaiser-Guttman rule.
581 *Psychol Rep* 68, 855–858.
- 582 King, A.J., Wilson, A.M., Wilshin, S.D., Lowe, J., Haddadi, H., Hailes, S., Morton, J., 2012.
583 Selfish-herd behaviour of sheep under threat. *Curr Biol* 22, R561-562.
- 584 Ligout, S., Foulquié, D., Sèbe, F., Bouix, T., Boissy, A., 2011. Assesment of sociality in farm
585 animals: the use of the arena test in lambs. *Appl Anim Behav Sci* 135, 57-62.
- 586 Lui, H.S., Shuley, N., 2006. Resonance based radar target identification with multiple
587 polarizations. Presented at the EEE Antennas and Propagation Society International Symposium.
- 588 Morand-Ferron, J., Cole, E.F., Quinn, J.L., 2015. Studying the evolutionary ecology of cognition
589 in the wild: a review of practical and conceptual challenges. *Biol Rev* 91, 367–389.
- 590 Pérez-Escudero, A., Vicente-Page, J., Hinz, R.C., Arganda, S., de Polavieja, G.G., 2014.
591 idTracker: tracking individuals in a group by automatic identification of unmarked animals. *Nat*
592 *Methods* 11, 743–748. <https://doi.org/10.1038/nmeth.2994>
- 593 Phocas, F., Boivin, X., Sapa, J., Trillat, G., Boissy, A., Le Neindre, P., 2006. Genetic correlations
594 between temperament and breeding traits in Limousin heifers. *Animal Science* 82, 805-811.
- 595 Poirier, J.R., Aubert, H., Jaggard, D.L., 2009. Lacunarity of rough surfaces from the wavelet
596 analysis of scattering data. *IEEE Transactions on Antennas and Propagation* 57, 2130–2136.
- 597 R Core Team, 2014. R: a Language and Environment for Statistical Computing, R Foundation for
598 Statistical Computing. ed. Vienna, Austria.
- 599 Redmon, J., Divvala, S., Girshick, R., Farhadi, A., 2016. You Only Look Once: Unified, Real-
600 Time Object Detection. *Proceedings of the IEEE Conference on Computer Vision and Pattern*
601 *Recognition* 779–788.
- 602 Reynolds, D.A., Rose, R.C., n.d. Robust text-independent speaker identification using Gaussian
603 mixture speaker models. *IEEE Transactions on Speech and Audio Processing* 3, 72–83.
- 604 Riley, J.R., Smith, A.D., Reynolds, D.R., Edwards, A.S., Osborne, J.L., Williams, I.H., Carreck,
605 N.L., Poppy, G.M., 1996. Tracking bees with harmonic radar. *Nature* 379, 29–30.

606 <https://doi.org/10.1038/379029b0>
607 Romero-Ferrero, F., Bergomi, M.G., Hinz, R.C., Heras, F.J.H., de Polavieja, G.G., 2019.
608 idtracker.ai: tracking all individuals in small or large collectives of unmarked animals. *Nature*
609 *Methods* 16, 179–182.
610 Ryan, H., 1994. Ricker, Ormsby, Klauder, Butterworth - A choice of wavelets. *CSEG Recorder*
611 8–9.
612 Simon, W., Klein, T., Litschke, O., 2014. Small and light 24 GHz multi-channel radar. Presented
613 at the IEEE Antennas and Propagation Society International Symposium (APSURSI).
614 Tomkiewicz, S.M., Fuller, M.R., Kie, J.G., Bates, K.K., 2010. Global positioning system and
615 associated technologies in animal behaviour and ecological research. *Philosophical Transactions*
616 *of the Royal Society B*. <https://doi.org/10.1098/rstb.2010.0090>
617 Voulodimos, A.S., Patrikakis, C.Z., Sideridis, A.B., Ntafis, V.A., Xylouri, E.M., 2010. A
618 complete farm management system based on animal identification using RFID technology.
619 *Computers and Electronics in Agriculture* 70, 380–388.
620 <https://doi.org/10.1016/j.compag.2009.07.009>
621
622

623 **Tables**

624

625 **Table 1:** Technical characteristics of the FMCW radar used for indoor tracking (Haderer
626 et al., 2008) and outdoor tracking (Simon et al., 2014).

627

Name	Indoor	Outdoor	Note
	tracking	tracking	
Operating frequency	77GHz	24GHz	This frequency is also called the <i>carrier frequency</i> of the frequency-modulated signal transmitted by the radar
Modulation Bandwidth	3GHz	800MHz	Frequency interval, centred at the operating frequency, used for the saw-tooth frequency modulation of the transmitted signal
Resolution	5cm	18.75cm	Resolution = $\frac{c}{2B}$, with c the celerity and B the modulation bandwidth
Ramp time	256 μ sec	1ms	Up-ramp duration of the saw-tooth frequency-modulated signal (or chirp duration)
Repetition time	50ms	30ms	Period of the transmitted frequency-modulated signal (or chirp repetition interval)
Number of linear arrays in the transmitting array antenna	4	1	One linear array composed of 8x2 rectangular patches radiating elements
Number of linear arrays in the receiving array antenna	8	2	Eight linear arrays composed of 8 rectangular patches radiating elements
Main lobe beamwidth of the transmitting array antenna in the horizontal plane	50°	58°	Angular range (or field of view) of the radar illumination in the horizontal plane
Transmitted power	100mW	100mW	Power delivered at the input terminals of the transmitting array

			antenna (the radiated power is defined as the product of the transmitted power by the efficiency of the antenna)
--	--	--	--

628

629

630

631

632

633 **Table 2:** Comparison of data processing characteristics with radar and video tracking

634 systems.

635

Tracking method	Radar	Video
Number of measures per second	50	25
Read Only Memory (ROM) for all measures of a sheep	151Mo	62Mo
Random Access Memory (RAM) per measure	524Kb	3.7Mb
Processing time per measure	<20ms	250ms
Total false detection rate	6%	16%

636

637

638 **Table 3:** Analyses of behavioural classes. Results of the best GLMM (binomial family,
 639 after model selection – see Table S1). The model tested the effects of phase, docility,
 640 weight, sex, age, sociability, and dual interaction of each variable with phase, on the
 641 proportion of time spent in fast movements (behavioural class 2). Sheep identity was
 642 included as a random factor. Significant effects ($p < 0.05$) are shown in bold.
 643

Variable	Estimate	z-value	P-value
Phase	-1.272453	-102.321	< 0.001
Docility	-0.134811	-2.725	0.006
Weight	0.042312	0.753	0.451
Sex	-0.018224	-0.165	0.869
Age	-0.095193	-1.673	0.094
Sociability	0.137659	3.596	< 0.001
Phase x docility	0.156352	19.868	< 0.001
Phase x weight	0.046431	5.223	< 0.001
Phase x sex	0.068090	3.882	< 0.001
Phase x age	0.078200	8.537	< 0.001
Phase x sociability	-0.127900	-20.900	< 0.001

644
 645
 646
 647 **Table 4:** Wavelet analyses. Results of the best GLMM (Poisson family, after model
 648 selection – see details in Tables S2 and S3). The model tested the effects of phase,
 649 docility, weight, sex, age, sociability, and binary interactions of each variable with phase,
 650 on the number of wavelets. Lamb identity was included as a random factor. Significant
 651 effects ($p < 0.05$) are shown in bold. Wavelet Y: longitudinal movements. Wavelet X:
 652 latitudinal movements.
 653

	Variable	Estimate	t-value	P-value
Wavelet	Phase	513.352	54.603	<0.001

Y	Sex	-11.392	-0.835	0.405
	Weight	2,417	0.349	0.727
	Age	-3,875	0,552	0.582
	Docility	-3.342	-0,548	0.585
	Sociability	17.371	3.679	<0.001
	Phase x sex	38.656	2.103	0.0403
	Phase x weight	1.941	0.208	0.836
	Phase x age	-2.426	-0.257	0.798
	Phase x docility	1.253	0.152	0.879
Wavelet	Phase	-67.0684	-5.68335	< 0.001
X	Sex	-2.70137	-0.21731	0.828
	Weight	-1.28441	-0.203557	0.839
	Age	-0.193189	-0.0302208	0.976
	Docility	-9.23551	-1.66137	0.100
	Sociability	0.669471	0.155654	0.877
	Phase x sex	27.8832	1.64681	0.106
	Phase x weight	-5.40654	-0.629084	0.532
	Phase x age	-1.34492	-0.154463	0.878
	Phase x docility	17.9056	2.36483	0.022
	Phase x sociability	7.0736	1.207	0.233

654

655

656 **Table 5:** Heatmap analyses. Results of the best GLMM (Poisson family, after model
657 selection – see details in Tables S4 and S5). The model tested the effects of phase,
658 docility, weight, sex, age, sociability, and dual interactions of each variable with phase,
659 on the number of areas where the lamb spent more than 1s. Sheep identity was
660 included as a random factor. Significant effects ($p < 0.05$) are shown in bold. A. Low
661 spatial resolution. B. High spatial resolution.
662

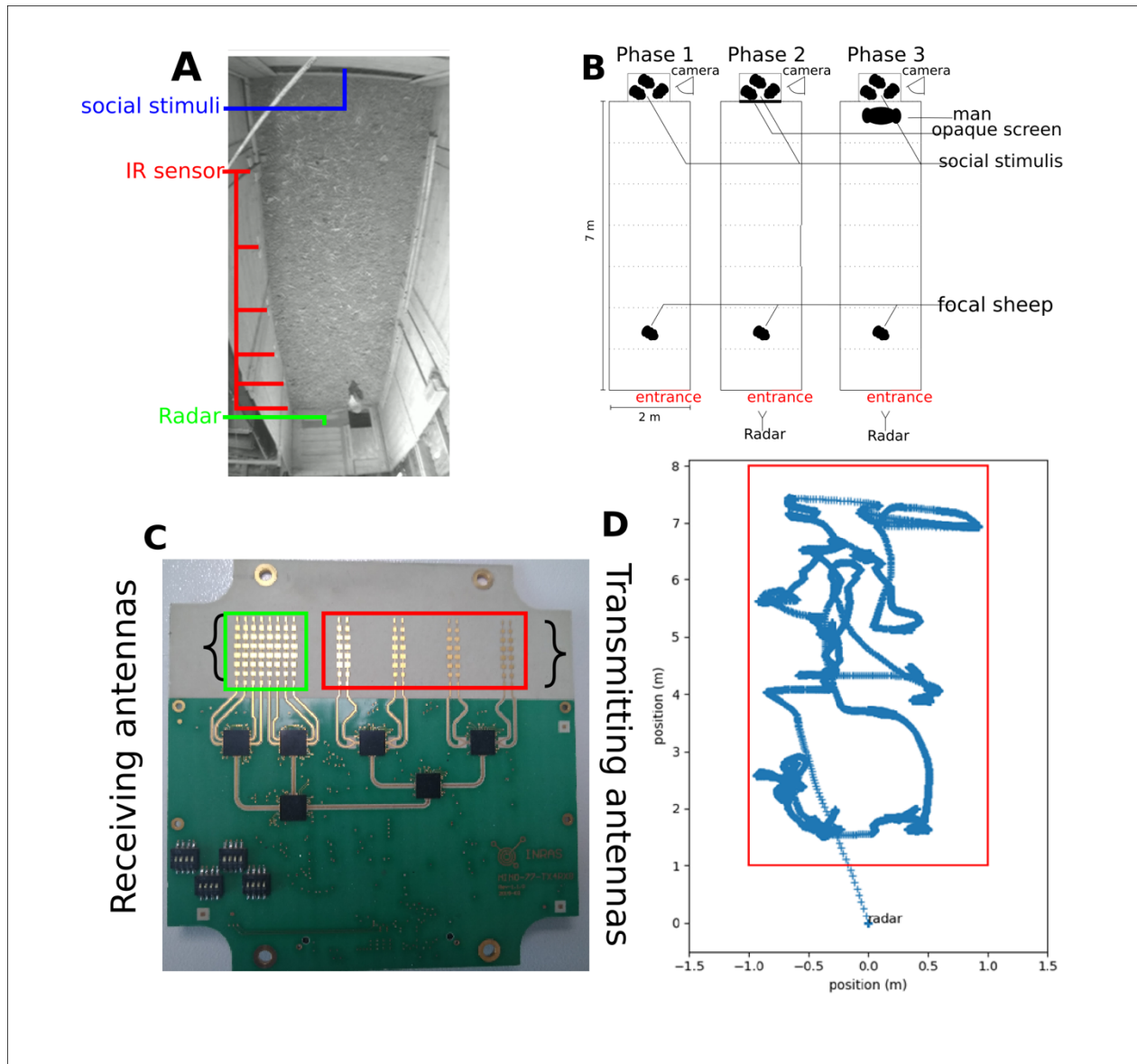
	Variable	Estimate	t-value	P-value
A	Phase	-0.597701	-9.20941	< 0.001
	Weight	0.0615106	1.99628	0.046
	Sociability	0.0365622	1.63703	0.102
B	Sex	0.0188161	0.299427	0.765
	Age	-0.0653912	-2.04381	0.041
	Phase	-0.765708	-14.4685	< 0.001
	Docility	-0.0837715	-2.665	0.008
	Sociability	0.0480015	2.19218	0.029
	Weight	0.0407016	1.27774	0.201
	Phase x docility	0.0978634	2.15262	0.031

663

664

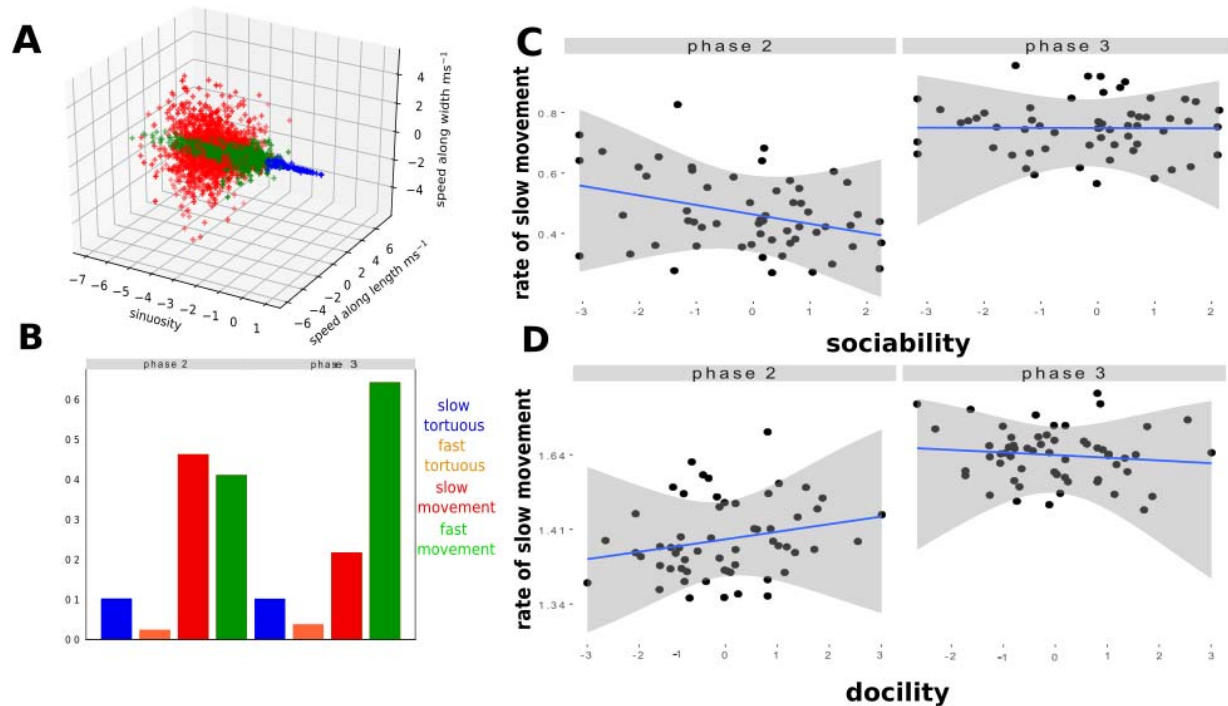
665 **Figures**

666



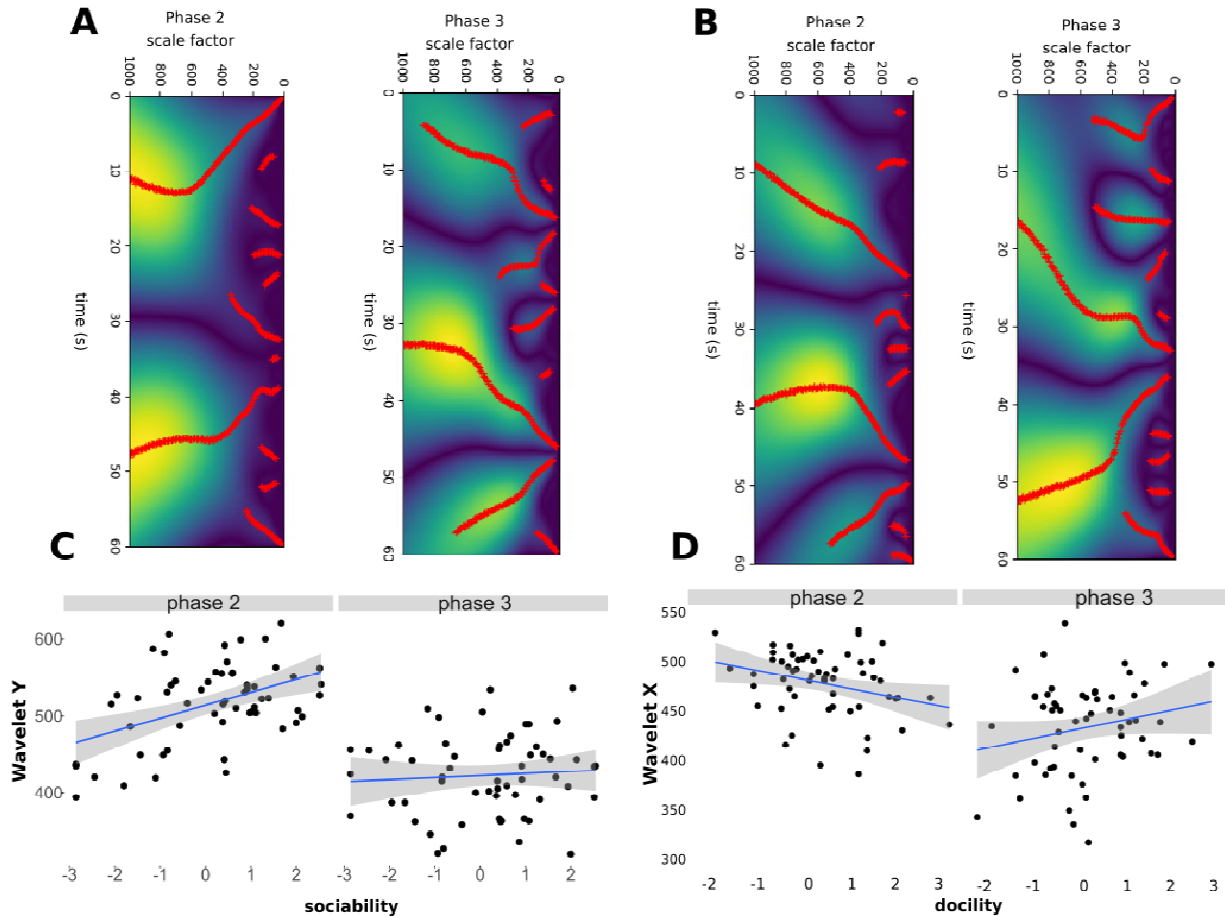
667
668

669 Figure 1: Corridor test. A. Top view of the focal sheep and the social stimuli in the
670 corridor (example image extracted from video data). B. schematic representation of
671 experiments phases 1, 2 and 3. C. Image of the FMCW radar frontend (phot credit AD).
672 Each rectangle corresponds to rectangular patch (Haderer et al., 2008). D. Example of
673 position estimations of a sheep over time after removing the clutter and normalizing the
674 estimated value.



675
676 **Figure 2:** Analyses of behavioural classes. A. Distribution of the four behavioural
677 classes after a Gaussian Mixture Model. B. Frequency of behavioural classes during
678 phase 2 and phase 3 of the corridor test. C. Correlation between the proportion of time
679 spent in slow movements and the sociability score of sheep during phase 2 and 3 (see
680 details of models in Table 3). D. Correlation between the proportion of time spent in slow
681 movements and the sociability score of sheep during phase 2 and 3 (Table 3). N = 64
682 sheep.
683

684



685

686 **Figure 3:** Wavelet analyses. A. Example of wavelet transform for lateral movements (X).

687 Red dots correspond to the detection of a change in the displacement at scale factor
688 and time position (i.e., a local maximum of the wavelet transform of the signal position).

689 B. Example of wavelet transform for longitudinal movements (Y). C. Relationship

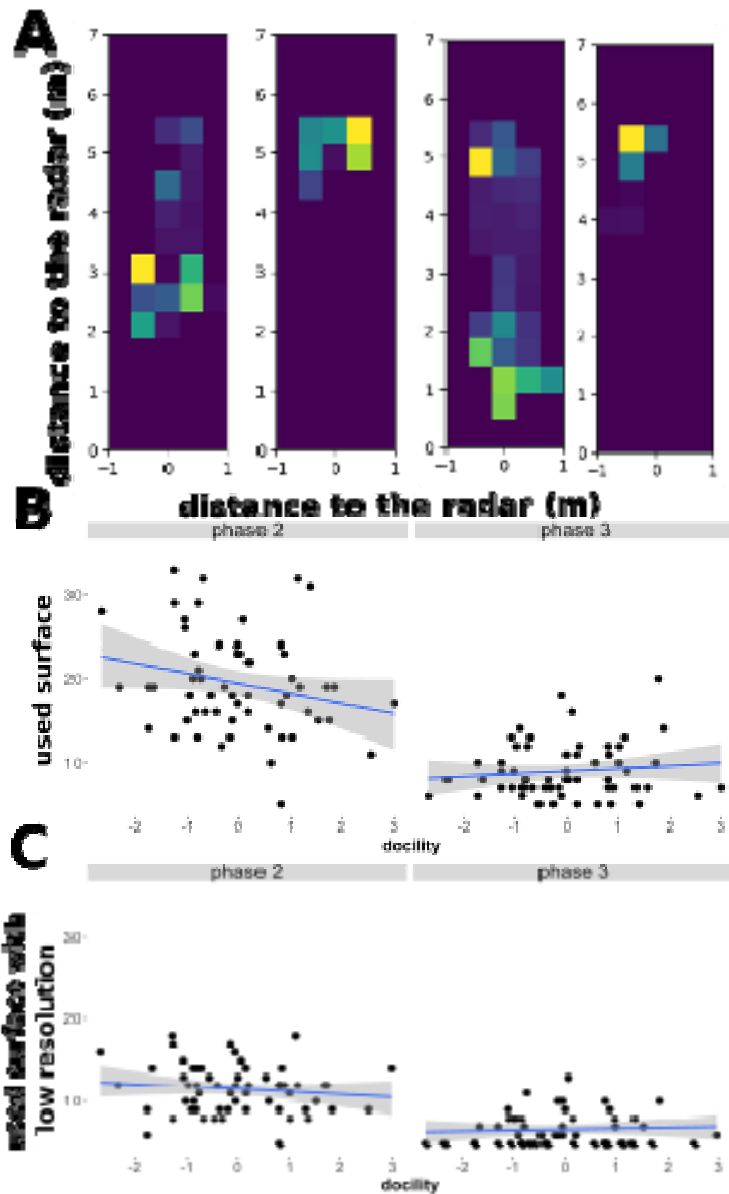
690 between the number of local maxima (red dots in Figures A and B) in the wavelet

691 extraction and the degree of sociability of sheep during phases 2 and 3. D. Relationship

692 between the number of wavelets and the degree of docility of sheep during phases 2

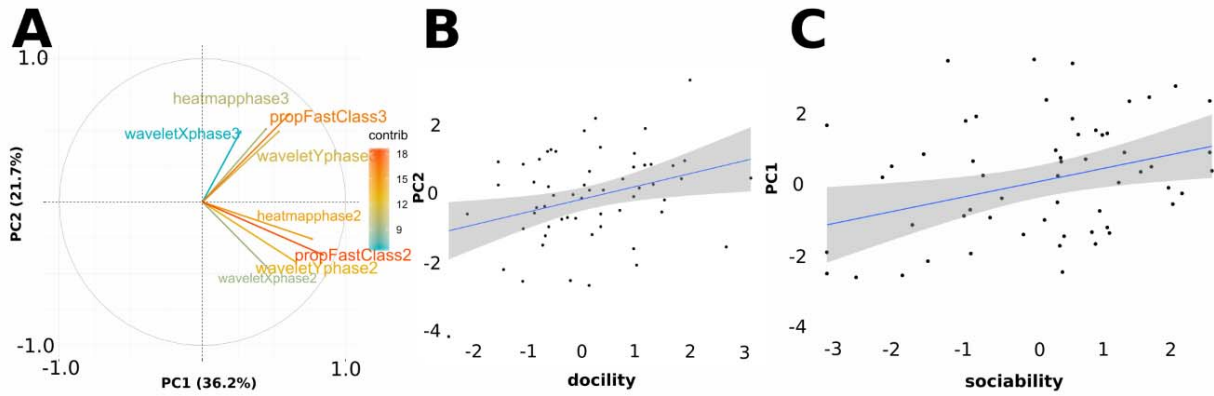
693 and 3. See details of models in Table 4. N = 64 sheep.

694



695
696 **Figure 4:** Heatmap analyses. Relationship between the number of zones occupied by
697 the lambs and the degree of docility in phase 2 and phase 3. A. Low spatial resolution
698 grid (cell dimension: 0.6 x 1m). B. High spatial resolution grid (cell dimension: 0.44 x
699 0.40 m). Top: examples of heatmaps. Bottom: Correlations. See details of models in
700 Table 6. N = 64 sheep.

701



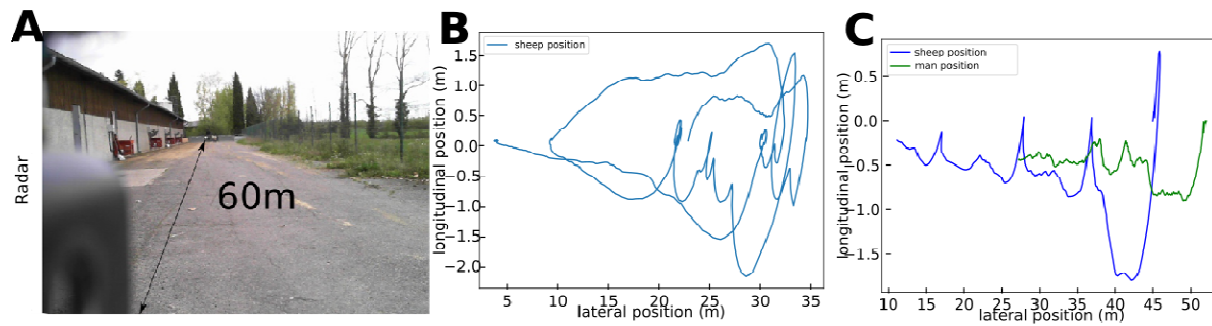
702

703

704 **Figure 5:** A. Correlations between the two first components (PCs) of the principal
705 component analysis (PCA). Arrows represent the eight behavioural variables on PC1
706 (movement speed) and PC2 (movement increase between phases). Contribution of
707 variables to the variance explained is colour coded. Each data point represents the PC1
708 and PC2 scores of a given lamb (N = 64). B. Relationship between PC1 and sociability.
709 C. Relationship between PC2 and docility. Blue lines represent linear models (see main
710 text). N = 64 sheep.

711

712



713

714 **Figure 6.** A. Picture of the outside corridor used for radar tracking of a sheep. The radar
715 was positioned 60m from the end of the corridor. B. Example of trajectory of a sheep
716 derived from radar data. C. Example of trajectory derived from radar data of a sheep
717 (red) and a man (green) to induce the sheep movement.

718

719

720 **Supplementary materials**

721

722 **Data S1:** Raw trajectories obtained from radar and video for each sheep.

723

724 **Table S1:** Model selection for behavioural class analyses. Null model, best model,
725 second and third best models are displayed.

Variables	AIC	Delta AIC	Weight
age x phase + weight x phase + docility x phase + sex x phase + sociability x phase	5423.774	0	9.92E-01
age x phase + weight x phase + docility x phase + sociability x phase	5433.82	10.04546	6.53E-03
age x phase + weight x phase + docility x phase + sex + sociability x phase	5436.306	12.5314	1.88E-03
Age x phase + docility x phase + sex x phase + sociability x phase	5447.138	23.36415	8.37E-06

726

727 **Table S2:** Model selection for X wavelet analyses (latitudinal movements). Null model,
728 best model, second and third best models are displayed.

Variables	AIC	Delta AIC	Weight
age x phase + weight x phase + docility x phase + sex + sociability x phase	1170.346	0	5.93E-01
age + weight x phase + docility x phase + sex + sociability x phase	1173.937	3.591115	9.85E-02
age x phase + weight + docility x phase + sex + sociability x phase	1174.289	3.942563	8.26E-02
age x phase + weight + docility x phase + sex + sociability	1174.586	4.239789	7.12E-02

729
 730 **Table S3:** Model selection for Y wavelet analyses (longitudinal movements). Null model,
 731 best model, second and third best models are displayed.

Variables	AIC	Delta AIC	Weight
age x phase + weight x phase + docility x phase + sex + sociability x phase	1189.577	0	5.73E-01
age x phase + weight x phase + docility + sex + sociability x phase	1193.051	3.474946	1.01E-01
age x phase + weight + docility x phase + sex + sociability x phase	1193.325	3.748755	8.79E-02
age + weight x phase + docility x phase + sex + sociability x phase	1193.374	3.797822	8.57E-02

732
 733 **Table S4:** Model selection for heatmap analyses (low spatial resolution). Null model,
 734 best model, second and third best models are displayed.

Variables	AIC	Delta AIC	Weight
weight x phase + sociability x phase	544.1552	0	1.35E-01
weight x phase + sex x phase + sociability x phase	546.3065	2.151297	4.61E-02
sex x phase + sociability x phase	546.376	2.220815	4.46E-02
weight x phase + sociability x phase + docility x phase	546.569	2.413782	4.05E-02

736
 737 **Table S5:** Model selection for heatmap analyses (high spatial resolution). Null model,
 738 best model, second and third best models are displayed.

Variables	AIC	Delta AIC	Weight
age + docility x phase + weight x phase + sociability	664.2827	0	0.058719217
age + docility x phase + weight + sociability	664.9303	0.6476525	0.042476067

739

age + docility x phase + sociability x phase	665.5479	1.2652317	0.031191675
docility x phase + weight x phase + sociability x phase	665.8718	1.5891709	0.026527492

740

741

742